CHEMISTRY OF MATERIALS

ARTICLE

pubs.acs.org/cm

Fabrication of a Highly Conductive Ordered Porous Electrode by Carbon-Coating of a Continuous Mesoporous Silica Film

Hirotomo Nishihara,*,† Taeri Kwon,† Yu Fukura,† Wataru Nakayama,† Yasuto Hoshikawa,† Shinichiroh Iwamura,† Norikazu Nishiyama,‡ Tetsuji Itoh,§ and Takashi Kyotani†

†Institute of Multidisciplinary Research for Advanced Materials, Tohoku University, 2-1-1 Katahira, Aoba-ku, Sendai, 980-8577, Japan

‡Division of Chemical Engineering, Graduate School of Engineering Science, Osaka University, 1-3 Machikaneyama, Toyonaka, Osaka 560-8531, Japan

§National Institute of Advanced Industrial Science and Technology, 4-2-1 Nigatake, Miyagino-ku, Sendai, 983-8551, Japan

Supporting Information

ABSTRACT: A mesoporous silica film (MSF, 20 × 20 mm in size) with 3D accessible mesopores (*Fmmm* symmetry) was synthesized on a current collector substrate, and then the entire pore surface was coated with an extremely thin carbon layer. The resulting carbon-coated mesoporous silica film (C/MSF), which well retains the continuous silica phase with its ordered mesopore network intact, has many advantages over conventional MSFs, porous carbons, or carbon electrodes. Thanks to the continuous carbon-coated layer, C/MSF is electrically conductive, and besides, it has remarkably better stability in an aqueous solution than MSFs. These features enable C/MSF to be used as a stable electrode in aqueous electrolyte solutions. In addition, C/MSF exhibits a much higher rate of performance as an electrode of an electric double layer capacitor than conventional powdery electrodes, indicating that the C/MSF electrode has excellent electrical conductivity, which can be ascribed to the continuous film shape of C/MSF. Another noticeable feature of C/MSF is light transmittance (67.9% at a wavelength of 1000 nm). Thus, C/MSF can be a transparent porous electrode unlike any porous carbon electrodes ever reported. Furthermore, due to the uniform mesopores (2 nm in diameter), C/MSF showed a large capability of immobilizing a giant active species such as iron-porphyrin molecules. Indeed, a much larger current was detected for the charge transfer from C/MSF to the iron-porphyrin than in the case of the iron-porphyrin loaded on a conventional graphite electrode. C/MSF is therefore a promising candidate as an effective electrode in various fields.

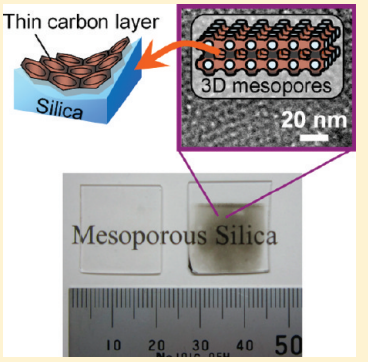

KEYWORDS: ordered mesoporous carbons, carbon-coated mesoporous silica, graphene, biosensors, artificial photosynthesis

INTRODUCTION

By using mesoporous silica as hard templates, ordered mesoporous carbons (OMCs) can be synthesized.[1,2] Unlike other mesoporous carbons such as mesoporous activated carbons[3] and carbon aerogels,[4] OMCs possess ordered an arrangement of uniform-sized mesopores, thereby having a significant potential as effective sorbents, catalyst supports, and electrodes.[5] Among them, the application to the electrochemical field is especially interesting and noteworthy because such an application is impossible for electrically insulative mesoporous silicas. As electrode materials, OMCs have been used for electric double layer capacitors,[2,6,7] lithium-ion batteries,[8−10] fuel cells,[11−13] biosensors,[14−17] and biofuel cells.[18] In many cases, OMCs exhibit better performances than conventional carbon-based electrodes due to such unique features of OMCs as uniform-sized mesopores, ordered mesopore connections, high surface area, and large mesopore volume.

It should be noted that OMCs are generally obtained as fine powders. Consequently, when OMCs are used as an electrode, they must be mixed with binder polymers and conductive additives to form an electrode sheet. The sheet thus prepared inevitably contains random macropores in the interparticle voids and shows a noticeable interparticle electric resistance. If it is possible to prepare a continuous OMC film on a large-size substrate, the film itself could be used as a porous electrode free from both random macropores and interparticle resistance. The film-shaped OMC can be synthesized by using thermoplastic polymers as templates, i.e., the so-called soft-template method.[19,20] For example, by using a microphase separation of a spin-coated diblock copolymer, Dai et al. synthesized an OMC film where arrayed cylindrical mesopores run vertically to the substrate. The microphase separation, however, does not allow the formation of mesopores with a diameter less than 30 nm. To prepare an OMC film with a smaller pore size, Nishiyama et al. used surfactant micelles as a template just like the case of the synthesis of mesoporous silicas. The resulting OMC film has *Fmmm* symmetry with 3D-connected mesopores with a diameter of 3 to 8 nm.[20,21] In these soft-template methods, a mesostructure composed of the following two phases is first formed: one phase made of a rigid thermosetting polymer will be converted

Received: November 26, 2010
Revised: April 22, 2011
Published: June 13, 2011

into carbon, and the other one made of a thermoplastic polymer or a surfactant will play the role of a template. The organic−organic composite thus obtained is then heat-treated under an inert atmosphere to remove the template phase and, at the same time, to convert the thermosetting polymer into carbon. During the heat-treatment step, the framework structure noticeably shrinks with the temperature and the framework ordering appreciably decreases as a result, although such a high temperature treatment is inevitable to achieve the high electrical conductivity enough for an electrode. For instance, by a heat-treatment up to 1073 K, the periodicity of the OMC film decreased to 34% of its original value.[21] Another problem is the poor controllability of pore structure: the structure variety and regularity of OMC films are much lower than those of mesoporous silica films (MSFs).

In contrast to OMC films, there are many reports on the synthesis of the MSFs with a variety of 3D accessible pore structures, such as cubic ($Im\bar{3}m$, $Pm\bar{3}m$, and $Pm3n$),[22,23] hexagonal ($P6_3/mmc$),[22−24] and orthorhombic ($Fmmm$).[25] In addition, MSFs are optically transparent. If the entire mesopore surface of a continuous MSF can be uniformly coated with an extremely thin (less than 1 nm) carbon layer, the resulting carbon-coated MSF becomes endowed with electrical conductivity but keeps its inherent ordered 3D pore structure and transparency. Of course, such a continuous film has neither random macropores nor interparticle resistance. Moreover, it should be quite easy to tailor its pore structures according to the need of each application because the already established methodologies for the pore-controlling of MSFs can be used. Besides, carbon-coating may bring the improvement of chemical stability. Though silica is generally not very stable in aqueous solutions, especially under basic conditions, the carbon-coated surface is expected to exhibit better stability. Such a property is significantly important for electrode materials since an electrode is often used in an aqueous electrolyte solution.

We have previously proposed a new method that enables a perfect carbon-coating of the entire pore surface of mesoporous silica (SBA-15) powder with an extremely thin (less than 1 nm) carbon layer.[26] In this work, we apply the carbon-coating technique to a large (20 × 20 mm) MSF formed on a current collector substrate and examine how much the carbon-coating is uniform in such a large silica film. We then use the resulting carbon-coated MSF (C/MSF) directly as an electrode and evaluate its performance in terms of electrical conductivity, long-term stability, and mass-transfer properties inside the continuous mesopore network. Furthermore, we load a giant active material such as iron-porphyrin molecules into the uniform mesopores in C/MSF to confirm its electron transfer ability to the active material.

EXPERIMENTAL SECTION

Preparation of Carbon-Coated Mesoporous Silica Film (C/MSF). Figure 1 shows the preparation procedure of C/MSF. As a current collector substrate, a Pt−Ti sputtered silicon wafer (20 × 25 mm in size) was used. The Pt layer plays a role of a current pass, and the Ti layer is a binder of silicon and Pt. The continuous MSF with the 3D accessible pore (space group is $Fmmm$) was synthesized onto the substrate with a vapor infiltration technique.[25] First, a mixture solution of Brij56, water, ethanol, and sulfuric acid (molar ratio is 0.16:100:50:0.9) was prepared. After dropping the solution (0.1 mL) on the substrate, the substrate was rotated at 4000 rpm for 60 s for spin coating. The resulting substrate coated with the surfactant micelles was

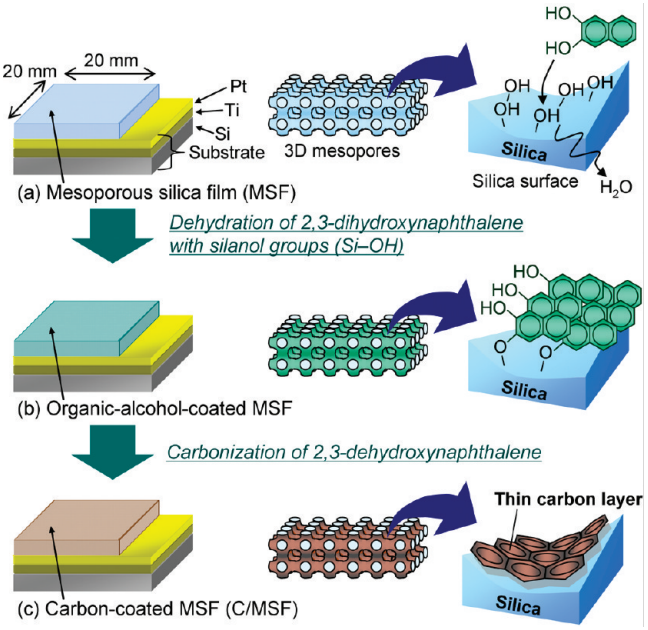

Figure 1. Preparation procedure of the carbon-coated mesoporous silica film (C/MSF). (a) Continuous MSF (space group is $Fmmm$) formed on a current collector substrate. Illustrations for the mesopore structure and the mesopore surface of MSF are presented. Note that the illustration of the mesopores is a simplified one and does not exactly correspond to the actual structure. On the mesopore surface of MSF, there are a lot of silanol groups (−OH). (b) An organic-alcohol-coated MSF. (c) C/MSF.

vertically placed in a closed bottle (40 mL in volume) along with a mixture of TEOS (0.1 mL) and 5 M HCl (0.1 mL). Note that the substrate was kept from the mixture in the bottle. The bottle was then placed in an oven at 333 K for 15 min. During this period, the TEOS vapor is infiltrated into the surfactant micelles together with a hydrolysis catalyst (HCl), and a firm silica matrix is formed as a result. Finally, the surfactant was removed by calcination at 673 K for 5 h to obtain the continuous MSF (Figure 1a). Before the spin coating, one end (5 × 20 mm) of the substrate was covered with a polyvinyl chloride tape to prevent the coating of MSF onto this part. The uncoated part was used as an electric connection terminal.

Carbon-coating was carried out by the method reported elsewhere.[26] In short, 2,3-dihydroxynaphthalene (DN) was introduced on the pore surface of MSF through a dehydration reaction of a hydroxyl group of DN with a silanol group of the silica at 573 K (Figure 1b). Then, DN introduced on the silica surface was carbonized under Ar flow up to 1073 K (its heating rate was 5 K min^{-1}) for 4 h and the carbon-coated MSF (referred to as C/MSF, Figure 1c) was obtained.

To evaluate the transmittance of the C/MSF layer, a similar C/MSF was prepared also onto a quartz plate (its thickness is 1 mm) as a separate experiment.

Loading of Porphyrin to C/MSF. A solution was prepared by dissolving 2,3,7,8,12,13,17,18-ocataethyl-*21H,23H*-porphine iron(III) chloride (FeOEP, 30 mg) in ethanol (25 mL), and then C/MSF attached to the substrate was immersed into the solution. By drying the substrate at 313 K for 30 min, FeOEP-loaded C/MSF was obtained.

Characterizations. The cross-section of the C/MSF attached to the substrate was observed with a scanning electron microscope (SEM; Hitachi S-4800). To characterize the long-range structure regularity of the film samples, X-ray diffraction (XRD) patterns were measured with a Shimazu XRD-6100 apparatus with Cu−Kα radiation generated at 30 kV and 20 mA. The ordered mesoporous structures of MSF and

dx.doi.org/10.1021/cm103388y |*Chem. Mater.* 2011, 23, 3144–3151

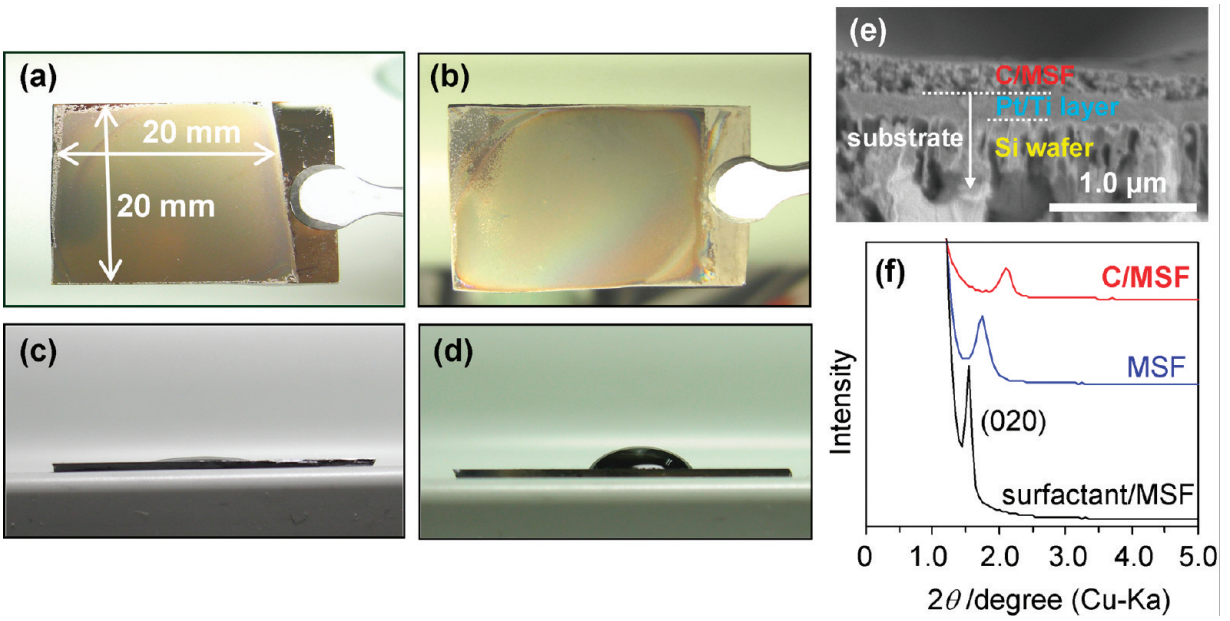

Figure 2. Photographs of (a) MSF and (b) C/MSF formed on the substrates, together with water droplets attached on (c) MSF and (d) C/MSF. The range of MSF deposited is 20 × 20 mm. (e) A SEM image of the cross-section of C/MSF/substrate. (f) XRD patterns of as-synthesized MSF (surfactant/MSF), MSF after the surfactant removal (MSF), and C/MSF. Each pattern was directly measured by using the film sample attached to the substrate.

C/MSF were observed by a transmission electron microscope (TEM; JEOL, JEM-2010), using an acceleration voltage of 200 kV. Before the observation, the film samples were physically separated from the substrate with a diamond pencil. The carbon layer formed onto MSF was characterized with a Raman spectrometer (JASCO, NRS-3300) with a 532.2 nm line. In addition, the carbon was liberated from MSF by immersion in HF (47%) solution for 6 h, and the isolated carbon layer was subjected to TEM observation. The amount of carbon embedded in porous silica is generally estimated by weight loss during its combustion with a thermal gravimetric analyzer. However, the amount of carbon in the C/MSF/substrate is too small (ca. 0.02 wt %) to detect the weight loss of carbon. Thus, we estimated the carbon amount with a temperature programmed oxidation (TPO) technique in the following manner:[27] C/MSF/substrate was heated at a linear heating rate of 4 K min^{-1} up to 1273 K under an oxidizing gas flow (5 vol % O_2 in He), and the gases (CO_2 and CO) evolved from the film were quantitatively analyzed with a gas chromatograph (GC; GL Science Inc., Cp-2002). From the total amount of carbon emitted, the carbon amount in C/MSF was calculated. The surface electrical resistivity of a pristine substrate, MSF/substrate, and C/MSF/substrate were measured by a four-probe technique with Loresta-GP MCP-T610 equipment (Mitsubishi Chemical Co.). The transmittance of the C/MSF layer formed on a quartz plate was evaluated with a UV/vis spectrometer (JASCO, V-670).

Electrochemical Measurements. C/MSF with the substrate was directly used as a working electrode. It was immersed into an electrolyte solution (1 M H_2SO_4 or 1 M NaCl), and then, the electrolyte solution was impregnated into C/MSF under reduced pressure for 1 h at 313 K. After the vacuum impregnation, the C/MSF/substrate was kept in the electrolyte solution for several hours before the electrochemical measurements. The electrochemical measurements were conducted with a three-electrode cell, which is equipped with a working electrode (C/MSF), a counter electrode (Pt mesh), and a reference electrode (Ag/Ag^+, RE-IC; BAS inc.). Before the electrochemical measurements, the electrolyte solution was bubbled with N_2 gas to remove dissolved O_2. Cyclic voltammograms were measured with a potentiostat/galvanostat (Hokuto Denko Corporation, Hz-500) in 1 M H_2SO_4 or 1 M NaCl electrolyte solutions at 298 K. The gravimetric capacitance [F g^{-1}] was calculated by dividing the obtained capacitance [F] by the total amount [g] of C/MSF used for cyclic voltammetry. For the FeOEP-loaded C/MSF, cyclic voltammetry was carried out with almost the same setting except for a different electrolyte solution (1 M KCl aq).

RESULTS AND DISCUSSION

Morphology of C/MSF and Its Ordered Mesopore Structure. Figure 2a and b shows photographs of MSF and C/MSF, respectively, formed on the current collector substrates. The color of MSF is translucent gray, and it becomes a little darker upon carbon-coating. Though MSF and C/MSF have nonuniform fringes which were formed by spin-coating (Figures 2a and b), C/MSF looks smooth and has a continuous face except for the fringe part. To examine the hydrophobicity of the carbon-coated surface, a contact angle of a water droplet was measured on both MSF and C/MSF. In MSF, the water droplet was completely dispersed due to the strong hydrophilicity of silica (Figure 2c), but the water droplet attached on C/MSF kept a contact angle of about 55°, indicating the increase in hydrophobicity by carbon-coating (Figure 2d). The contact angle on C/MSF is, however, smaller than that of the pure graphite surface (>90°). One of the reasons for the smaller angle may be the low degree of crystallinity of the resulting carbon (note that the carbonization temperature is as low as 1073 K). Figure 2e shows a SEM image of the cross-section of C/MSF. A continuous C/MSF layer (its thickness is about 200 nm) is firmly attached to the very flat surface of a Pt/Ti layer, a current pass layer. We observed such a smooth contact between C/MSF and the Pt/Ti layer throughout the substrate without any voids or cracks, thus expecting a sufficient electrical connection between these two layers.

Figure 2f shows XRD patterns of as-synthesized MSF (with the surfactant remaining in MSF), MSF after surfactant removal

dx.doi.org/10.1021/cm103388y |*Chem. Mater.* 2011, 23, 3144–3151

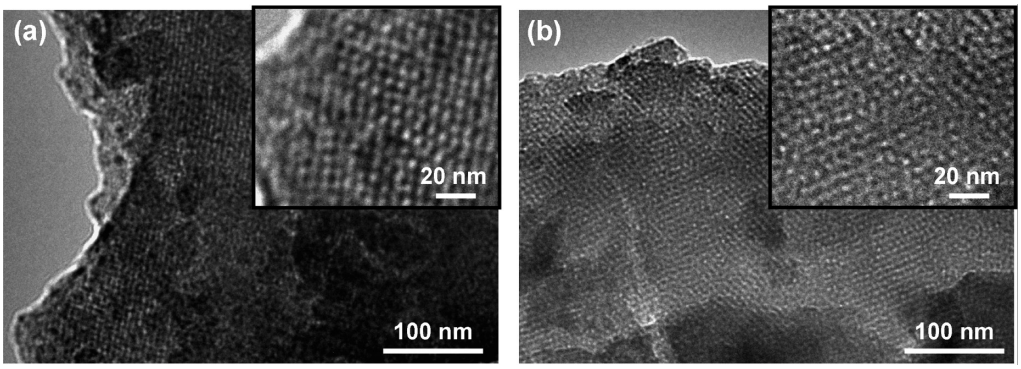

Figure 3. TEM images of (a) MSF and (b) C/MSF. Each sample was physically liberated from the substrate before the observation. Insets are the corresponding high resolution images.

(MSF), and C/MSF. All the samples show a peak derived from (020) planes of the *Fmmm* structure.[25] The *d*-spacing of the (020) planes, $d_{(020)}$, of the as-synthesized MSF can be calculated to be 5.70 nm. Upon surfactant removal at 673 K, the *d*-spacing becomes 5.06 nm. Further heat-treatment at 1073 K in the carbon-coating process decreases its value down to 4.20 nm. Though the present MSF was found to slightly shrink with the heat-treatment, the contraction is much smaller than that in the case of OMS films synthesized with a soft-template method.[21] To illustrate, in the case of OMS films with the same *Fmmm* structure as the present silica, their (010) planes shrink to 34% upon carbonization at 1073 K,[21] but the present C/MSF shrinks no more than 26%. Song et al. have recently reported an easy approach to improve the robustness of OMC films by the addition of silica to a matrix.[28,29] In their method, contraction can be decreased with increasing the silica content. For a *Fmmm* structure film, they succeeded in reducing the film contraction from 65% to 35% of its original value upon carbonization at 1073 K, by introducing silica up to 74 wt %.[29] However, the precursor of the present C/MSF comprises a pure silica framework coated with organic alcohol molecules, and therefore, contraction by heating was as low as that in the case of pure MSFs.[30] Such smaller contractions are effective in reducing the distortion of the ordered mesopore morphology, resulting in retaining a sharp mesopore size distribution.[28,29]

The MSF and C/MSF layers were peeled off from the substrate and subjected to TEM observation (Figure 3). In both samples, ordered mesopore structures are clearly observed, which is in accordance with the XRD results (Figure 2f). In addition, we confirmed from the SEM observation that the mesopores are open up to the outside surface of the MSF and C/MSF, and there is no deposition of extra carbon such as grains and particles outside the C/MSF (see Supporting Information). From the TEM (Figure 3b) and SEM images (Figure S1b, Supporting Information) of C/MSF, its mesopore diameter can be estimated to be ca. 2 nm.

Thin Carbon Layer Deposited on the Silica Surface. From the TPO experiment, the carbon amount can be calculated to be 24.9 wt % in C/MSF. If this large amount was not used for the coating of the mesopores but placed only on the outside surface of MSF, there must be noticeable fractions of carbon matter as grains and/or particles. However, this is not the case, as indicated by the TEM (Figure 3b) and SEM (Figure S1b, Supporting Information) images. We therefore conclude that the carbon introduced into MSF exists inside the mesopores. Moreover, since the mesopore sizes of C/MSF in the TEM image (Figure 3b) look very uniform, it is likely that the carbon does not plug the mesopores but uniformly covers the mesopore surface.

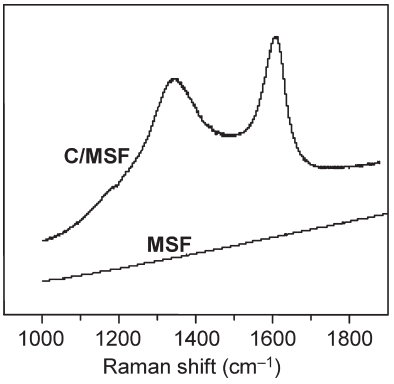

Figure 4. Raman spectra of MSF and C/MSF recorded with 532.2 nm laser line.

In order to examine the connectivity of the carbon layer, C/MSF was immersed into a 47% HF solution, and the silica framework was removed. If the carbon layer was not continuous, the carbon could not have retained the whole film shape upon the removal of the silica framework, and it could have been broken into small fragments. However, we do not observe any visible change on the film sample before and after the HF etching. In addition, the SEM observation (data is not shown) revealed that the film sample remains firmly attached to the substrate like Figure 2e. These findings are strong evidence that the carbon layer is well connected in the mesopore network of MSF. The structure of the liberated carbon is further discussed in Supporting Information.

Figure 4 shows the Raman spectra of MSF and C/MSF formed onto Si wafers. MSF shows an inclined baseline with no scattering peak, but C/MSF clearly shows two peaks, the so-called D-band (1350 cm^{-1}) and G-band (1610 cm^{-1}), both of which are typical of carbonaceous materials. The intense G-band directly proves the significant presence of graphene sheets. The position of the intense G-band (1610 cm^{-1}) is a little higher than that of the graphite G-band (1580 cm^{-1}), suggesting that the graphene sheets in C/MSF are not developed like graphite and that they may be nanometer-sized sheets.[31,32]

Long-Term Stability in an Aqueous Solution. In general, mesoporous silica is not very stable in aqueous media, especially

dx.doi.org/10.1021/cm103388y |*Chem. Mater.* 2011, 23, 3144–3151

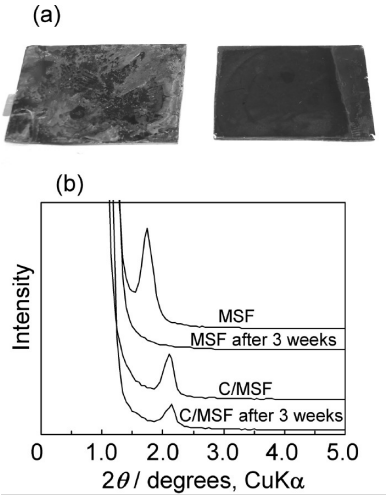

Figure 5. (a) Photographs of MSF (left) and C/MSF (right) after immersion into 1 M NaCl aqueous solution for 3 weeks. (b) XRD patterns of MSF and C/MSF before and after the immersion test.

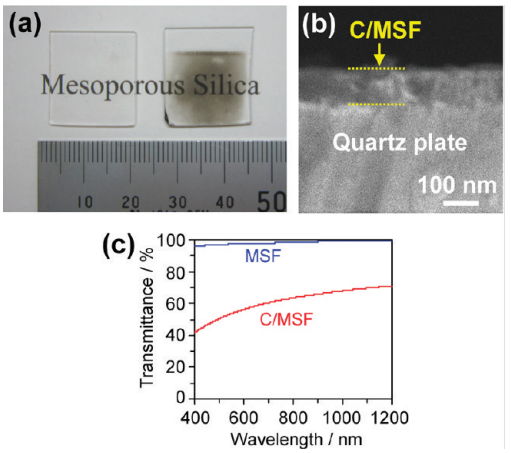

Figure 6. (a) Photographs of MSF (left) and C/MSF (right) formed on the quartz plates. One end of each plate was not covered with the mesoporous layer. (b) A SEM image of the cross-section of C/MSF/quartz. (c) Transmittance of the MSF and C/MSF on the quartz plates.

under basic conditions, because silica has some solubility in water. Even at neutral pH, amorphous silica can be dissolved at ordinary temperature to the extent of 100−150 ppm.[33] In the case of the present MSF, its amount is only 0.128 mg on one substrate (20 × 20 mm in area), and just a little over 1 mL of water is large enough to dissolve this small amount of silica. Brinker et al. indeed reported that MSF is almost dissolved in pH 7.4 aqueous solution within 1 day.[34] Such poor durability restricts its practical use in the electrochemical field, e.g., in biosensors and biofuel cells because an electrode material in such applications is usually used in an aqueous solution. However, C/MSF is expected to have better chemical stability than the pristine silica, if the whole surface of silica is covered with a carbon layer. We thus examined the chemical stability of C/MSF. Figure 5a shows photographs of MSF and C/MSF after immersion into a 1 M NaCl aqueous solution for 3 weeks. Note that we choose this solution because it will be used as an electrolyte for electrochemical measurements as described later. MSF looks extremely eroded even just by the immersion into the neutral media, whereas C/MFS remains almost intact. Figure 5b shows XRD patterns of MSF and C/MSF before and after the immersion test. As was expected from Figure 5a, the structure of MSF was completely destroyed and lost its regularity upon 3 weeks immersion in 1 M NaCl. In marked contrast, C/MSF retains the ordered structure even after the long-term test due to the protecting surface carbon layer. Though the carbon layer is not tough enough against HF etching, it is sufficient to inhibit the dissolution of silica into an aqueous electrolyte with neutral pH, which has been often used for electrochemical applications in many cases.

Surface Electrical Resistivity. The surface electrical resistivities of the pristine substrate, MSF, and C/MSF were measured with a four-probe method. The resistivity of the pristine substrate was 4.00×10^{-2} Ω/□, which is low enough as a current collector, due to the conductive Pt and Ti metal layers. After the formation of insulative MSF on the substrate (Figure 1a), the resistivity is significantly increased to 1.90×10^{7} Ω/□. Upon carbon-coating (Figure 1c), the large resistivity is, however, remarkably decreased to almost the same value (4.04×10^{-2} Ω/□) as that of the pristine substrate. The excellent conductivity of C/MSF indicates that the carbon layer on the silica mesopore surface is continuous throughout the whole MSF. Though it is possible to endow a mesoporous silica film with proton conductivity by loading $CsHSO_4$,[35] it is almost impossible to achieve such a high electrical conductivity as in the case of C/MSF simply by adding any molecular additives to silica.

Light Transmittance. To evaluate the transmittance of the C/MSF layer, C/MSF was prepared also onto a quartz plate. Figure 6a shows photographs of such MSF and C/MSF. The original MSF looks completely transparent, and interestingly, C/MSF also has some transparency. From the cross-section SEM image (Figure 6b), the thickness of C/MSF was estimated to be ca. 100 nm. Figure 6c shows the transmittance of MSF and C/MSF. At a wavelength of 1000 nm, C/MSF has a transmittance of 67.9%, which is close to the value of a transparent graphene film (70.7%) with the thickness of ca. 10 nm.[36]

C/MSF shows transparency because it does not contain very large amounts of carbon. However, the small amount of carbon forms an extremely thin continuous layer to cover most of the silica surface, which endows C/MSF with both a sufficient chemical stability and a high electrical conductivity. Accordingly, the amount of carbon in C/MSF is well balanced to exhibit not only chemical stability and electrical conductivity but also transparency. These three characteristics make C/MSF distinctive from conventional porous carbon electrodes which are in principle completely black and are not suitable for photochemical applications.

Inner Resistance and Mesopore Network Connection. Next, we tried to use the as-synthesized C/MSF on the current collector substrate directly as an electrode. Figure 7 shows cyclic voltammograms of C/MSF and the pristine substrate, measured in 1 M NaCl and 1 M H_2SO_4 electrolyte solutions. In Figure 7a, C/MSF exhibits higher current than the pristine substrate, indicating that the presence of C/MSF increases the electric double layer capacitance. In other words, C/MSF has a larger amount of electrically conductive surface area than the pristine substrate. In the acidic electrolyte solution (Figure 7b), we observed again the increase in capacitance upon the formation of C/MSF, but in this electrolyte, the pristine substrate shows an increase of cathodic current below 0.1 V, which can be regarded as the chemisorption of H^+ onto the Pt surface.[37,38] Interestingly,

dx.doi.org/10.1021/cm103388y |*Chem. Mater.* 2011, 23, 3144–3151

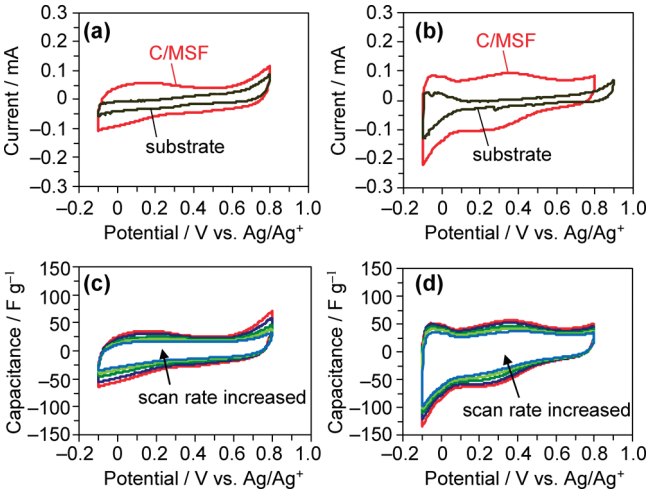

Figure 7. (a,b) Cyclic voltammograms of C/MSF (red line) and the pristine substrate (black line) measured in (a) 1 M NaCl and (b) 1 M H_2SO_4. Scan rate was 10 mV s^{-1}. (c,d) Cyclic voltammograms of C/MSF measured in (c) 1 M NaCl and (d) 1 M H_2SO_4 at elevated scan rates of 10, 20, 50, 100, and 200 mV s^{-1}.

such a cathodic current can be observed also in C/MSF. This indicates that the electrolyte solution passed through the 3D pores of the C/MSF layer and then reached the Pt surface. Figures 7c and d show the cyclic voltammograms of C/MSF at elevated scan rates (note that the *y*-axis is expressed as a gravimetric capacitance). From Figures 7c and d, the gravimetric capacitances of C/MSF are estimated to be ca. 30 and 50 F g^{-1} in 1 M NaCl and 1 M H_2SO_4 respectively, and these values are comparable to those of carbon-coated mesoporous silica (SBA-15) powder (25 and 39 F g^{-1} in 1 M NaCl and 1 M H_2SO_4, respectively).[39] Since the electric double-layer capacitance is proportional to the surface area of an electrode material, it is possible to estimate the surface area of C/MSF from its double-layer capacitance. This approach allows one to determine the surface area of a sample with a very small amount, like the case of C/MSF. Note that we have actually tried to measure the specific surface area of C/MSF with the conventional nitrogen physisorption technique; however, it was not possible due to the very small amount of C/MSF: the weight of C/MSF of 20 × 20 mm area is only 0.1 mg. Considering that the double-layer capacitance of carbon-coated mesoporous silica is 0.07 F m^{-2} in 1 M NaCl,[39] the specific surface area of C/MSF can be estimated to be as high as 429 m^2 g^{-1}. The appearance of the sufficient capacitance also indicates that the electrical contact between the Pt surface and C/MSF is very well though the thickness of the carbon layer is very thin.

It is noteworthy that, in both c and d in Figure 7, the shapes of the voltammograms are almost unchanged even at higher scan rates. This finding indicates that the inner resistance of the C/MSF electrode is very small due to its continuous film shape. Previously, we have prepared carbon-coated mesoporous silica (SBA-15) powder[26] and measured its cyclic voltammograms in 1 M NaCl and 1 M H_2SO_4.[39] Since the carbon-coated SBA-15 (C/SBA-15) is a powdery form, a sheet electrode was prepared by mixing C/SBA-15 with a PTFE binder and a conductive additive (carbon black). Then the sheet electrode was attached to a Pt mesh as a current corrector. The resulting cyclic voltammograms are shown in Figure 8, where the capacitance of C/SBA-15, in both electrolytes, significantly drops with increasing the

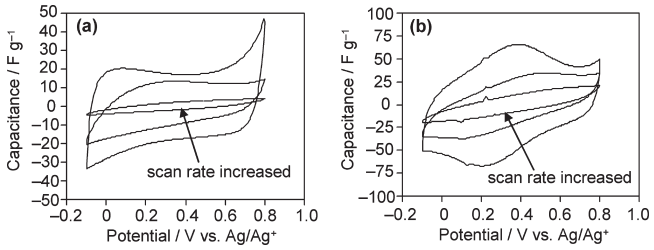

Figure 8. Cyclic voltammograms of C/SBA-15 measured with the three-electrode cell in (a) 1 M NaCl and (b) 1 M H_2SO_4. Scan rates were 1, 10, and 50 mV s^{-1}. Reprinted with permission from ref 39. Copyright 2010 Elsevier.

scan rate up to 50 mV s^{-1} due to a large inner resistance, making a striking contrast with C/MSF, which can keep the capacitance even up to 200 mV s^{-1} (Figures 7c and d). This remarkable difference between C/MSF and C/SBA-15 can be ascribed to their different morphologies. In the conventional electrode sheets composed of porous carbon powders, the inner resistance of the electrode is the sum of the several resistance components, such as (i) contact resistance between the current collector and the electrode sheet, (ii) interparticle resistance of carbon powders, (iii) inner resistance of carbon, and (iv) ion-transfer resistance inside the carbon nanopores. Since both C/MSF and C/SBA-15 are carbon-coated mesoporous silicas and in principle should have similar nanostructures, the components (iii) and (iv) of C/MSF are not very different from those of C/SBA-15. However, from its film shape, C/MSF has advantages as for (i) and (ii). As is evident from Figure 2e, the C/MSF layer is firmly attached to the current corrector, making component (i) very small. In addition, C/MSF is completely free from component (ii). Thus, forming a continuous film is a very effective way to prepare a highly conductive porous electrode with fast electrochemical response.

Performance As a Support of an Active Material. Judging from the 3D network of the ordered and continuous mesopores, the high chemical stability in aqueous media, transparency, and the excellent electrical conductivity, C/MSF can be a promising electrode for various applications such as biosensors,[40,41] microbial fuel cells,[42] and artificial photosynthesis.[43] For these applications, high capability of immobilizing an active material and smooth charge transfer from the electrode surface to the loaded active material are indispensable. We thus examined the performance of C/MSF as a support for such active materials. Considering the mesopore diameter of C/MSF (ca. 2 nm), we chose 2,3,7,8,12,13,17,18-octaethyl-*21H,23H*-porphine iron(III) chloride (FeOEP, the molecular structure is shown in the inset of Figure 9, and its diameter is ca. 1.3 nm) as a model active material, and the cyclic voltammogram of the FeOEP-loaded C/MSF electrode was measured in 1 M KCl solution (Figure 9). Note that FeOEP does not dissolve in water so that there is no FeOEP desorption from the C/MSF electrode. A pair of well-defined redox peaks was clearly seen in Figure 9. This was attributed to the F(III)/F(II) redox couple coordinated in the porphyrinic ring.[44,45] The peak split between the anodic and cathodic peak potentials (ΔE_p) was 110 mV, which is similar to the conventional graphite electrode modified with iron porphyrins.[45] It is noteworthy that the intensity of the redox peaks (>0.1 mA) is greatly larger than that of the graphite electrode (<5 μA),[45] indicating that a considerably large amount of porphyrin can be reduced/oxidized on C/MFS. From the reduction current, the amount of electrochemically active FeOEP per geometrical electrode area (2 × 2 cm^2) is

dx.doi.org/10.1021/cm103388y |*Chem. Mater.* 2011, 23, 3144–3151

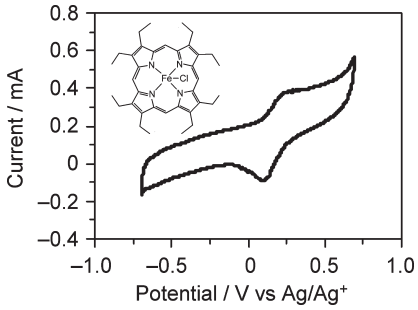

Figure 9. Cyclic voltammogram of FeOEP-loaded C/MSF measured in 1 M KCl aqueous solution in the absence of O_2. Potential range was −0.7 to 0.7 V. Scan rate was 10 mV s^{-1}. The inset is the molecular structure of FeOEP.

estimated to be 1.03×10^{-8} mol cm^{-2}. However, in the case of the graphite electrode, the maximum amount of electrochemically active porphyrin was no more than ca. 8×10^{-10} mol cm^{-2},[45] which corresponds to the monolayer adsorption amount on the entire surface of the graphite electrodes. Moreover, it was reported that further loading of porphyrin produced no further increase in the current.[45] Thus, C/MSF can be an effective platform which can hold a very large amount of electrochemically active giant active species, thereby being promising as highly sensitive sensors.

By using the present carbon-coating strategy, it is possible to prepare various types of continuous film electrodes with different pore morphologies and different pore diameters, depending on the needs of the applications. Moreover, the uniform mesopore size of C/MSF is expected to immobilize and stabilize biomolecules whose sizes are just fit to the mesopore.[46,47] C/MSF has therefore a great potential to be an effective electrode in various application fields.

CONCLUSIONS

A continuous mesoporous silica film (MSF) having 3D accessible mesopores (*Fmmm* structure) with a large area of 20 × 20 mm was prepared on a current collector substrate, and then uniform carbon-coating was conducted on MSF. Despite the carbon coating at a relatively high temperature of 1073 K, the resulting carbon-coated MSF (C/MSF) well retained the ordered mesoporous structure without large thermal shrinkage, thanks to the robust silica framework. Upon carbon coating, the surface of MSF became hydrophobic, and more importantly, its long-term stability in a neutral aqueous solution was remarkably improved. C/MSF exhibited excellent electrical conductivity and can be directly used as an electrode without any binders and conductive additives, both of which are always necessary in the case of porous carbon powders. The C/MSF electrode showed a considerable amount of electric double layer capacitance, and moreover, the capacitance of C/MSF did not drop very much with increasing the scan rate, revealing a remarkably low inner resistance of C/MSF compared to the conventional powdery electrodes. Furthermore, a large amount of iron-porphyrin could be loaded into C/MSF and clear charge transfer from C/MSF to the iron-porphyrin was demonstrated. In addition, the transmittance of the C/MSF layer is close to that of the transparent graphene electrode, making C/MSF a transparent porous electrode unlike any porous carbon electrodes ever reported. It can therefore be concluded that C/MSF is a promising candidate as an effective electrode in various fields, such as biosensors, microbial fuel cells, and artificial photosynthesis.

ASSOCIATED CONTENT

Supporting Information. SEM images of the top views of the film samples and TEM analysis of the liberated carbon from MSF. This material is available free of charge via the Internet at http://pubs.acs.org.

AUTHOR INFORMATION

Corresponding Author
*Fax: +81-22-217-5626. E-mail: nisihara@tagen.tohoku.ac.jp.

ACKNOWLEDGMENT

This research was partially supported by the Ministry of Education, Science, Sports and Culture, Grant-in-Aid for young scientists (B), 21750203.

REFERENCES

(1) Ryoo, R.; Joo, S. H.; Jun, S. *J. Phys. Chem. B* **1999**, *103*, 7743.
(2) Lee, J.; Yoon, S.; Hyeon, T.; Oh, S. M.; Kim, K. B. *Chem. Commun.* **1999**, 2177.
(3) Tamai, H.; Kakii, T.; Hirota, Y.; Kumamoto, T.; Yasuda, H. *Chem. Mater.* **1996**, *8*, 454.
(4) Hanzawa, Y.; Kaneko, K.; Pekala, R. W.; Dresselhaus, M. S. *Langmuir* **1996**, *12*, 6167.
(5) Ryoo, R.; Joo, S. H.; Kruk, M.; Jaroniec, M. *Adv. Mater.* **2001**, *13*, 677.
(6) Xing, W.; Qiao, S. Z.; Ding, R. G.; Li, F.; Lu, G. Q.; Yan, Z. F.; Cheng, H. M. *Carbon* **2006**, *44*, 216.
(7) Yoon, S.; Lee, J. W.; Hyeon, T.; Oh, S. M. *J. Electrochem. Soc.* **2000**, *147*, 2507.
(8) Fan, J.; Wang, T.; Yu, C. Z.; Tu, B.; Jiang, Z. Y.; Zhao, D. Y. *Adv. Mater.* **2004**, *16*, 1432.
(9) Hu, Y. S.; Adelhelm, P.; Smarsly, B. M.; Hore, S.; Antonietti, M.; Maier, J. *Adv. Funct. Mater.* **2007**, *17*, 1873.
(10) Zhou, H. S.; Zhu, S. M.; Hibino, M.; Honma, I.; Ichihara, M. *Adv. Mater.* **2003**, *15*, 2107.
(11) Choi, W. C.; Woo, S. I.; Jeon, M. K.; Sohn, J. M.; Kim, M. R.; Jeon, H. J. *Adv. Mater.* **2005**, *17*, 446.
(12) Joo, S. H.; Choi, S. J.; Oh, I.; Kwak, J.; Liu, Z.; Terasaki, O.; Ryoo, R. *Nature* **2001**, *412*, 169.
(13) Su, F. B.; Zeng, J. H.; Bao, X. Y.; Yu, Y. S.; Lee, J. Y.; Zhao, X. S. *Chem. Mater.* **2005**, *17*, 3960.
(14) Lu, X. B.; Xiao, Y.; Lei, Z. B.; Chen, J. P.; Zhang, H. J.; Ni, Y. W.; Zhang, Q. *J. Mater. Chem.* **2009**, *19*, 4707.
(15) You, C. P.; Xuewu, Y.; Wang, Y.; Zhang, S.; Kong, J.; Zhao, D. Y.; Liu, B. H. *Electrochem. Commun.* **2009**, *11*, 227.
(16) Zhou, M.; Ding, J.; Guo, L. P.; Shang, Q. K. *Anal. Chem.* **2007**, *79*, 5328.
(17) Zhou, M.; Shang, L.; Li, B. L.; Huang, L. J.; Dong, S. J. *Biosensors Bioelectron.* **2008**, *24*, 442.
(18) Zhou, M.; Deng, L.; Wen, D.; Shang, L.; Jin, L. H.; Dong, S. J. *Biosensors Bioelectron.* **2009**, *24*, 2904.
(19) Liang, C. D.; Hong, K. L.; Guiochon, G. A.; Mays, J. W.; Dai, S. *Angew. Chem., Int. Ed.* **2004**, *43*, 5785.
(20) Tanaka, S.; Nishiyama, N.; Egashira, Y.; Ueyama, K. *Chem. Commun.* **2005**, 2125.
(21) Tanaka, S.; Katayama, Y.; Tate, M. P.; Hillhouse, H. W.; Miyake, Y. *J. Mater. Chem.* **2007**, *17*, 3639.
(22) Zhao, D. Y.; Yang, P. D.; Margolese, D. I.; Chmelka, B. F.; Stucky, G. D. *Chem. Commun.* **1998**, 2499.
(23) Zhao, D.; Yang, P.; Melosh, N.; Feng, J.; Chmelka, B. F.; Stucky, G. D. *Adv. Mater.* **1998**, *10*, 1380.
(24) Tolbert, S. H.; Schaffer, T. E.; Feng, J. L.; Hansma, P. K.; Stucky, G. D. *Chem. Mater.* **1997**, *9*, 1962.

(25) Maruo, T.; Nagata, K.; Nishiyama, N.; Egashira, Y.; Ueyama, K. *J. Colloid Interface Sci.* **2008**, *328*, 120.
(26) Nishihara, H.; Fukuraa, Y.; Inde, K.; Tsuji, K.; Takeuchi, M.; Kyotani, T. *Carbon* **2008**, *46*, 48.
(27) Aso, H.; Matsuoka, K.; Tomita, A. *Energy Fuels* **2003**, *17*, 1244.
(28) Song, L.; Feng, D.; Lee, H. J.; Wang, C.; Wu, Q.; Zhao, D.; Vogt, B. D. *J. Phys. Chem. C* **2010**, *114*, 9618.
(29) Song, L.; Feng, D.; Campbell, C. G.; Gu, D.; Forster, A. M.; Yager, K. G.; Fredin, N.; Lee, H. J.; Jones, R. L.; Zhao, D.; Vogt, B. D. *J. Membr. Chem.* **2010**, *20*, 1691.
(30) Boissiere, C.; Grosso, D.; Lepoutre, S.; Nicole, L.; Bruneau, A. B.; Sanchez, C. *Langmuir* **2005**, *21*, 12362.
(31) Ferrari, A. C.; Robertson *J. Phys. Rev. B* **2000**, *61*, 14095.
(32) Ferrari, A. C.; Robertson *J. Phys. Rev. B* **2001**, 64.
(33) Iler, R. K. *The Chemistry of Silica*; John Wiley & Sons: New York, 1979.
(34) Dunphy, D. R.; Singer, S.; Cook, A. W.; Smarsly, B.; Doshi, D. A.; Brinker, C. J. *Langmuir* **2003**, *19*, 10403.
(35) Otomo, J.; Wang, S.; Takahashi, H.; Nagamoto, H. *J. Membr. Sci.* **2006**, *279*, 256.
(36) Wang, X.; Zhi, L. J.; Mullen, K. *Nano Lett.* **2008**, *8*, 323.
(37) Ross, P. N. *Surf. Sci.* **1981**, *102*, 463.
(38) Conway, B. E. *Electrochemical Supercapacitors, Scientific Fundamentals and Technological Applications*; Kluwer Academic/Plenum Press: New York, 1999.
(39) Kwon, T.; Nishihara, H.; Fukura, Y.; Inde, K.; Setoyama, N.; Fukushima, Y.; Kyotani, T. *Microporous Mesoporous Mater.* **2010**, *132*, 421.
(40) Wohlstadter, J. N.; Wilbur, J. L.; Sigal, G. B.; Biebuyck, H. A.; Billadeau, M. A.; Dong, L. W.; Fischer, A. B.; Gudibande, S. R.; Jamieson, S. H.; Kenten, J. H.; Leginus, J.; Leland, J. K.; Massey, R. J.; Wohlstadter, S. J. *Adv. Mater.* **2003**, *15*, 1184.
(41) Yuan, J. H.; Wang, K.; Xia, X. H. *Adv. Funct. Mater.* **2005**, *15*, 803.
(42) Chaudhuri, S. K.; Lovley, D. R. *Nat. Biotechnol.* **2003**, *21*, 1229.
(43) Wasielewski, M. R. *Chem. Rev.* **1992**, *92*, 435.
(44) Yoshimoto, S.; Tada, A.; Itaya, K. *J. Phys. Chem. B* **2004**, *108*, 5171.
(45) Shlgehara, K.; Anson, F. C. *J. Phys. Chem.* **1982**, *86*, 2776.
(46) Fukushima, Y.; Kajino, T.; Itoh, T. *Curr. Nanosci.* **2006**, *2*, 211.
(47) Urabe, Y.; Shiomi, T.; Itoh, T.; Kawai, A.; Tsunoda, T.; Mizukami, F.; Sakaguchi, K. *ChemBioChem* **2007**, *8*, 668.